08,12,11,14

Monolithization of UHMWPE Reactor Powders

© Yu.M. Boiko[1], A.K. Borisov[1], D.V. Grankin[2], E.M. Ivan'kova[3], V.A. Marikhin[1], L.P. Myasnikova[1,¶], V.L. Preobrazhenskii[4], E.I. Radovanova[1], V.I. Siklitsky[1], T.D. Shidlovskii[1], M.M. Tsygankov[1]

[1] Ioffe Institute,
St. Petersburg, Russia
[2] Gwint Consulting Inc. Toronto,
Canada, Reno / the USA
[3] Branch of Petersburg Nuclear Physics Institute named by B.P. Konstantinov of National Research Centre „Kurchatov Institute" — Institute of Macromolecular Compounds,
St. Petersburg, Russia
[4] Connector Optics LLC,
St. Petersburg, Russia

¶ E-mail: Liuba.Myasnikova@mail.ioffe.ru

Received July 14, 2025
Revised July 16, 2025
Accepted July 17, 2025

The possibility of obtaining mechanically coherent films (precursors for subsequent strain hardening) from reactor powders of ultra-high molecular weight polyethylene (UHMWPE) synthesized on supported modified Ziegler-Natta and metallocene catalysts was studied. The compaction pressure at room temperature, as well as the temperature and sintering time of the compacts were varied. A comparative study of the fine structure of powders, their thermodynamical properties, molecular mobility in near-surface nanolayers, and their changes during monolithization under various temperature-time conditions was conducted. It is shown that in the optimal mode, UHMWPE powders synthesized on a Ziegler-Natta catalyst are better compacted and sintered than UHMWPE powders synthesized on a metallocene catalyst. Structural and kinetic criteria for the suitability of reactor powders for monolithization are discussed.

Keywords: reactor powder, ultra-high molecular weight polyethylene, compaction/sintering, plasma-induced thermoluminescence, differential scanning calorimetry, scanning electron microscopy, precursors for strain hardening.

DOI: 10.61011/0000000000

1. Introduction

An ultra-high molecular weight polyethylene (UHMWPE) is a very promising material due to a combination of unique physical properties (high wear resistance, resistance to aggressive media, a low friction coefficient, high impact strength, hydrophobicity, a low brittleness temperature as well as possibility to produce of high-strength high-modulus fibers from it, which are used in bulletproof jackets). At the same time, viscosity of the UHMWPE melt η_o, which obeys the known power law $\eta_o = M_w^{3/4}$ [1] and exceeds that of the conventional low-density polyethylene melt by 2−3 orders, makes it impossible to process the UHMWPE melt with $M_w > 10^6$ g/mol by traditional methods, such as die extrusion or hot pressing.

In order to produce ultra-high-strength high-modulus UHMWPE fibers, a gel-technology method was designed and commercialized in the 80s in the Netherlands, in which fibers were spun from a weakly-concentrated UHMWPE solution in a decalin with subsequent strain hardening of the gel-crystallized fibers [2]. Since it is costly and environmentally unfriendly, a solution-free („dry") method for producing ultra-strong, high-modulus film threads directly from UHMPE synthesis products, so-called reactor powders (RP), is now actively developing in the world. This method consists of sintering the RP at a temperature below the melting point of the PE, followed by orientational drawing of the monolithized material.

The initial idea of creating RP most suitable for dry processing was formulated by P. Smith *et al.*, who showed that if PE is synthesized at low temperature, a polymer with a low density of molecular entanglements is obtained, which can then be drawn to high degree of orientation drawing and obtain an oriented film thread with mechanical characteristics no worse than gel fibers [3,4].

This is where the concept of the RP of such nascent PE arose as a powder with extended chain crystals (ECC). Although, this study was only an impracticable demonstration of synthesis capabilities, but it was a trigger that activated a worldwide work of synthesis chemists to search for a correct catalyst and real synthesis conditions, which produced the good reactor powder suitable for monolithization and subsequent effective orientational hardening. Already in 2012, the Tejin-Aramid company (the Netherlands) could master a solid-phase method of processing the UHMWPE reactor powders into quite high-strength and high-modulus Endumax tapes, which however were inferior in strength σ

($\sigma = 2.5$ GPa) to the Dyneema fibers ($\sigma = 3.6$ GPa) that were produced by the gel technology by the company DSM (the Netherlands) and Spectra (Honeywell, USA). In laboratory conditions, both abroad [5,6] and in Russia [7–11], the oriented UHMWPE threads with much better mechanical characteristics were obtained from UHMWPE RP synthesized on post- metallocene catalysts. The strength of the film threads was up to 4.0 GPa, while a modulus of elasticity was up to 200 GPa. The similar results were obtained for the film threads of the UHMWPE reactor powders that were synthesized on catalysts modified by Mg compounds [11].

An assumption of the low density of entanglements of the ECC reactor powders was criticized in subsequent studies. It was discovered that the most reactor powders that were synthesized on both supported and metallocene various catalysts exhibit a complicate hierarchical supramolecular structure, whose elementary morphological unit were lamellas. It was found that very important were such parameters of the reactor powders, as a particle shape, particle sizes, size distribution of the particles, a green density of the powder and morphological units formed during synthesis [9,12].

At the same time, as shown in practice, achievement of the high strength characteristics depends not only on a structure of the RP particles, which is optimal for orientational drawing, but also on a capability of creating strong cohesive bonds between the particles, which prevent premature rupture of the sample during drawing until the maximum possible degree of drawing is reached.

Despite a large number of the studies for solid state processing of UHMWPE RP into the strong film fibers, a particle sintering mechanism is still understudied and there is no algorithm for preparing precursors from the reactor powders. In this case it is important to preserve the minimum number of entanglements existed in the original structure. Their number depends on a polymerization temperature, a catalyst type and many other synthesis conditions [12–14].

The present study was aimed at comparative investigating physical and mechanical properties of the precursors for strain hardening, which were produced in different conditions from the UHMWPE reactor powders synthesized on the various catalysts.

2. Experimental

2.1. Materials

The studies were carried out on:

1. Lab-scale UHMWPE reactor powder (Oz4838) that was synthesized on the postmetallocene catalysts by suspension polymerization in toluene as per a technique described in the study [6] and kindly provided to us by a Professor A.N. Ozerin (Institute of Synthetic Polymeric Materials, Moscow).

2. Lab-scale UHMWPE reactor powder (M3659) that was synthesized on the modified Ziegler-Natta titanium-magnesium catalyst (TMC) and kindly provided to us by Professor M.A. Mats'ko (Novosibirsk, Boreskov Institute of Catalysis).

The molecular weight of the Oz4838 reactor powder was $M_w = 4.4 \cdot 10^6$ g/mole, $T_{polym} = 40\,^\circ$C, the green density $\rho_{gd} = 0.083$ g/cm^3, the fraction $250 < d < 850\,\mu$m. This powder for the studies was selected on the basis of literature data that indicated formation of an optimal structure of the UHMWPE reactor powder, which was suitable for solid-phase processing [6]. The molecular weight of the reactor powder M3659 $= 3.5 \cdot 10^6$ g/mole, the green density $\rho_{gd} = 0.158$ g/cm^3.

2.2. Preparation of samples

The samples for the study were prepared according to a powder metallurgy principle, which has long been used in industry for high-melting metals, ceramics and insoluble and infusible polymers, such as polytetrafluoroethylene, polybenzimidazole, etc.

The scheme for preparing initial samples (precursors) for subsequent orientational hardening from the UHMWPE reactor powder includes two stages:

1. Compaction (monolithization) of the reactor powder at the room temperature to create the closest contact between the surfaces of the nearing neighboring UHMWPE RP particles and to increase adhesion strength of the compact due to the maximum possible reduction of free volume and removal of „trapped" air.

2. Sintering of the produced compact in order to create the largest number of cohesive bonds between the initial particles of the reactor powder, which provide mechanical strength of the precursor, which further allows strain hardening of the precursor by high-temperature multistage orientation drawing without premature rupture of the oriented sample along particle boundaries until it reaches the limiting orientational elongations. Sintering is carried out under the simultaneous action of pressure and temperature that does not exceed T_{melt} of the initial reactor powder.

2.2.1. Compaction

The first stage, which is RP compaction, was carried out by a cold pressing method (at the room temperature) using a specially made closed cylindrical mold of the internal diameter of 20 mm with two punches carefully adjusted to the diameter. The end surfaces of the plane-parallel punches were polished to a roughness of less than 1 μm.

For compaction, 30−35 mg of UHMWPE powder were placed between the punches and the mold was installed in a hydraulic press. Compaction was at the room temperature under the pressure $P \approx 50$ or 95 MPa for 15 min. Then, the press pressure was released. As a result, we produced the

initial compacted films of the diameter of $d = 20$ mm and the thickness of $h_1 = 0.10-0.18$ mm.

After compaction, both the UHMWPE powders (O4838 and M3659) become mechanically integral despite the fact that the M3569 compacts are still nontransparent (i. e. have micro-heterogeneities with sizes comparable to the light wavelength). The O4838 compacts are inhomogeneous: there are transparent and nontransparent places, apparently, because it is impossible to uniformly distribute the powder in the mold.

2.2.2. Sintering

The second stage, which is sintering of the compacted reactor powders, was carried out at the pressure of 95 MPa under various temperature conditions.

The film was placed in a mold heated to the required temperature, the pressured was increased to 95 MPa and the film was held under these conditions for 30 min. After that, the pressure was released, the film was removed and quickly cooled to the room temperature.

2.3. Differential scanning calorimetry

The samples were studied by differential scanning calorimetry (DSC) using a calorimeter DSC-500 „Spetspribor" (Russia) in a nitrogen atmosphere. A scanning rate was 1 K/min. In order to reduced systematic errors, thermal resistance of the samples and calorimetric capsules was minimized through a low weight of the samples (1–3 mg) and a low weight of the calorimetric capsules (16 mg).

2.4. Scanning electron microscopy

The structure of the reactor powders, the compacts and the sintered monolithic films and their cryocleavages was studied in a scanning-electron microscope SUPRA 55VP 32-49. In order to prevent accumulation of a charge on the surface of the particles, the latter were placed on special conducting substrates and covered by a thin Pt layers (of at most 10 nm thickness) by cathode sputtering. In order to reduce degradation effects on the polymer samples by electrons of a scanning electron probe, the studies were carried out at accelerating voltage of at most 5 kV. Resolution of the microscope at this voltage is at least 5 nm.

2.5. Plasma-induced thermoluminescence

Molecular mobility in nearsurface nanolayers of the compacted and sintered UHMWPE samples was studied using a Nanoluminograph that was recently designed in Ioffe Physical-Technical Institute and patented [15,16].

The samples of the studied powders were fastened in a vacuum chamber to a cylindrical holder cooled by liquid nitrogen. After vacuuming the chamber to the pressure of $1.33 \cdot 10^{-4}$ Pa and cooling the sample to 77 K, the chamber was pumped with argon to the pressure of 13.3 Pa and a high-frequency glowing discharge was ignited for 1 s (13.56 MHz) to activate a surface of an investigated sample. In order to minimize a modifying effect of plasma on the surface, the experimental discharge power was reduced to the value of 4 ± 0.1 mW/cm^3. The chamber was again pumped out to the pressure of 13.3 Pa and a photomultiplier tube (PMT) was used to record isothermal luminescence first and after a decline of its intensity to a PMT noise level holder heating was switched on and dependences of luminescence intensity on the temperature were recorded (the so-called glowing curves). We used the PMT Hamamatsu R-6095 (Japan) operating in a mode of counting single-electron pulses, with a maximum of sensitivity within the range from 400 to 600 nm. Noise intensity was reduced by cooling the PMT to 5 °C by means of a Peltier element. The glowing curves were recorded within the temperature interval from 77 to 300 K with linear heating of the sample at the rate of 10 K/min.

In order to prevent contamination of the surface of the studied samples with oil vapor from a forevacuum pump, the chamber was pumped out by means of an oil-free turbomolecular pump (HCube-80, Pfeiffer, Germany). The experimental conditions were identical for all the samples.

2.6. Mechanical tests

Due to a small size of the sintered films (about 20 mm in diameter), it was not possible to manufacture ordinary dumbbell-shaped samples used for GOST determination of mechanical characteristics in universal tensile machines. In order to measure strength of the precursors, the produced sintered films were cut into millimeter wide strips by means of a special device and their strength was measured by a Japanese universal tensile machine Shimadzu at the room temperature at a clamp extension speed of 10 cm/min.

3. Results and discussion

3.1. Differential scanning calorimeter

Thermogram analysis of the investigated compacts is needed primarily to determine a temperature, at which they can be sintered without changes of their internal structure (basically, not exceeding a temperature of deviation of a basic line from a horizontal). The thermograms were recorded at the same heating rate $v = 1$ K/min. Characteristics of an endothermic peak for the studied samples were compared — values of the temperature in the maximum of a melting peak, a width of the melting peak and a shape of an endothermic „shoulder" that is adjacent to the melting peak at the side of the low temperatures.

Figure 1 shows the thermograms of the compacted films.

It is clear that the melting temperatures of the studies UHMWPE reactor powders (140–141 °C) exceeds the equilibrium melting temperature of ordinary polyethylene

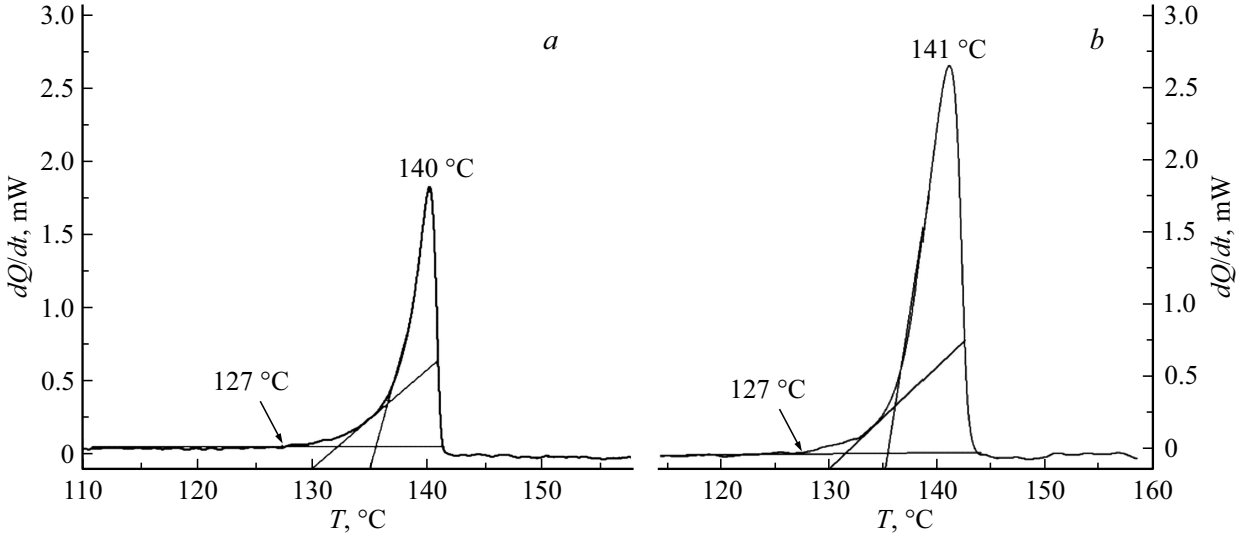

Figure 1. DSC thermograms of the compacts of the reactor powders *a*) M3659 and *b*) O4838.

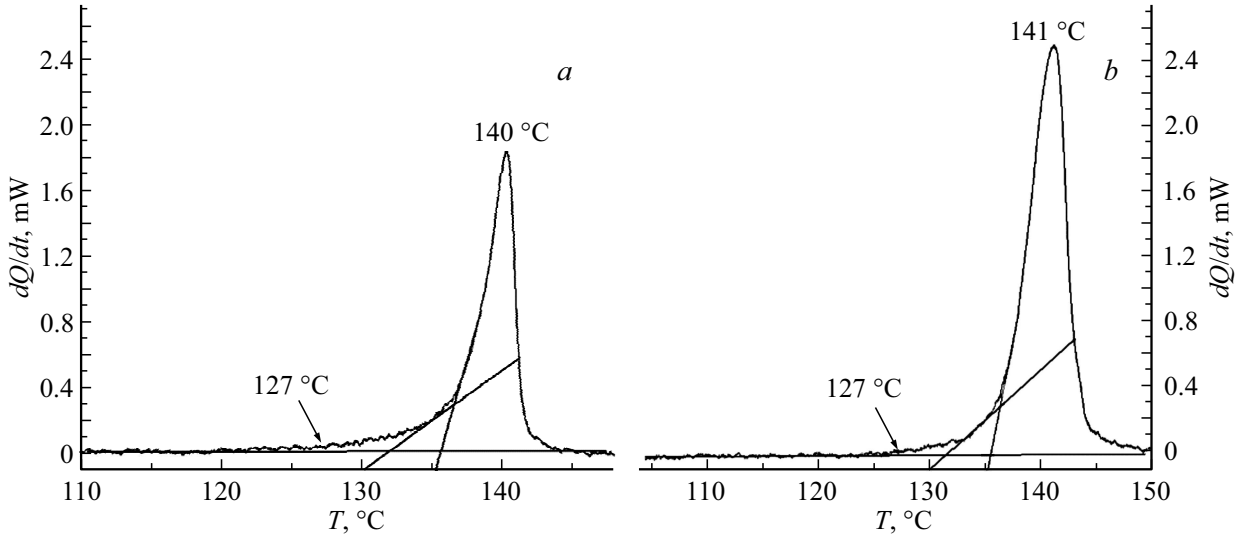

Figure 2. DSC thermograms of the samples sintered at 130 °C from the compacts of the reactor powders *a*) M3659 and *b*) O4838.

(135 °C), thereby indicating, as many authors believe, the low density of entanglements in the polymer [17]. It is known that sintering of the sample at the temperature above the melting temperature results in remelting of the initial structure with formation of folded crystals and in an incapability of achieving of high drawing degrees.

In the thermograms of both the compacted powders, the baseline starts deviating from the horizontal line at the temperature of 127 °C; at the temperature of 130 °C, defective or very small crystallites begin to melt, and at 135 °C, apparently, also defective, but larger crystallites start melting. However, the films sintered at 127 °C turned out to be quite brittle and further work with them was terminated. Since thermograms of the samples sintered at 130 °C under the pressure of 95 MPa practically did not change (Figure 2), which means the initial structure was not undesirably rebuilt in these conditions, all further experiments were carried out mainly with the UHMWPE samples sintered at 130 °C, 95 MPa for 30 min.

The choice of a sufficiently high sintering temperature for UHMWPE RP is driven by the desire to intensify the micro-Brownian motion of molecules at the boundaries between particles, which would seemingly increase the strength of the interparticle boundaries, since the healing mechanism involves the interdiffusion of molecular segments at the particle boundaries. At the same time, shear plastic strain can play a significant role in healing the boundaries. Measurement of the strength of the sintered samples (precursors) will allow us to evaluate a degree of healing of the interparticle boundaries of the precursors since it is these areas that are supposed to be destroyed first.

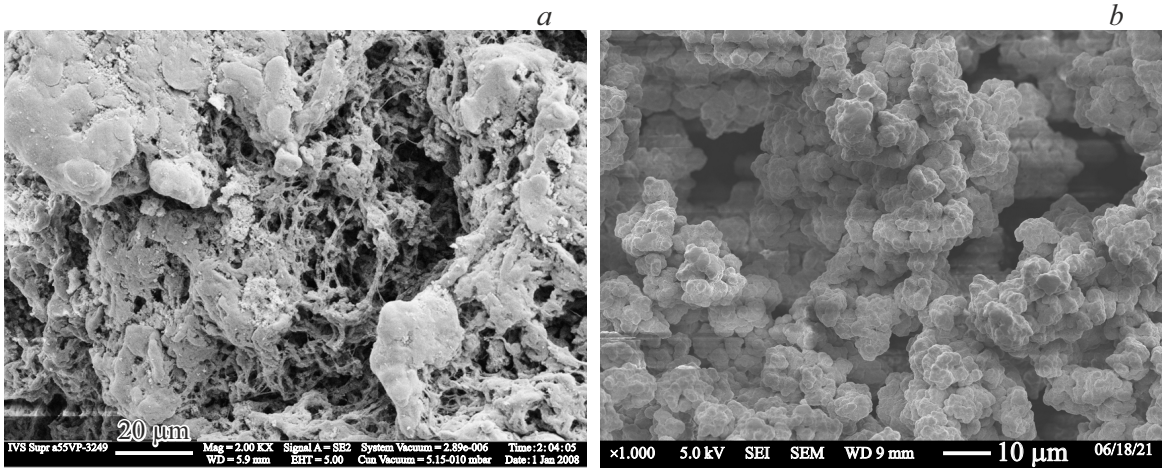

Figure 3. Micrographs of the particles of the reactor powders *a*) O4838 and *b*) M3659.

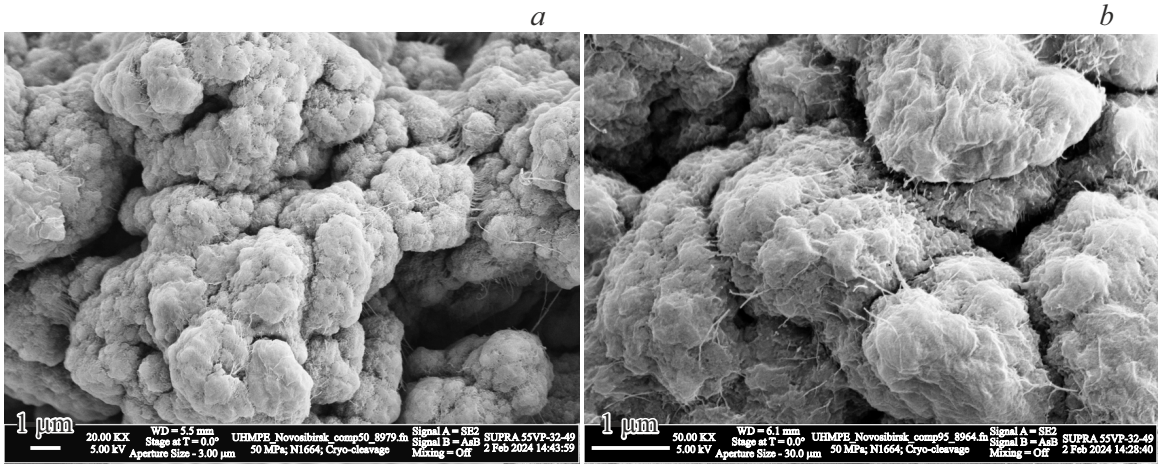

Figure 4. Cryo-cleavages of the compacts of the M3569 reactor powder, which are produced at the pressure of *a*) 50 MPa and *b*) 95 MPa.

3.2. Scanning electron microscopy

It is clearly seen in the micrograph of the separate particles at high magnifications that they have a complicate internal structure and consist of various morphological units: lamellar globules linked with fibrillar strands, lamellar stacks, separate fibrils, „shish-kebabs" etc. However, sizes, a number, a binding degree, integrity and mutual arrangement of these morphological formations are different in the various reactor powders.

The O4838 reactor powder (Figure 3, *a*) demonstrates a complex hierarchial morphology consisting of extended lamellas, lamellar crystals, fibrils and shish-kebabs, whereas the structure is loose and inhomogeneous.

The M3659 reactor powder (Figure 3, *b*) exhibits a quite dense structure of lamellar globules interlinked by few fibrillar strands.

In order to obtain information about interaction of the reactor powders particles during cold pressing and sintering, we have investigated a structure of a surface of particle cleavages obtained by fracture at the liquid nitrogen temperature of $-196\,^{\circ}$C.

Figure 4 shows micrographs of the cryo-cleavages of the studied compacts.

It is clear from the given micrographs that almost no link appeared between the morphological formations in the compacts of the M3569 reactor powder that were produced at 50 MPa (Figure 4, *a*). At the same time, in compacts obtained under a pressure of 95 MPa, fibrillar strands are visible between the lamellar globules, which apparently formed during compact fracture (Figure 4, *b*), which means that cohesive bonds could have formed between the globules under pressure under the influence of shear forces.

In compacts of RP O4838 with flake-like particles, many more bonds were formed during compaction, which is noticeable by the broken fibrillar formations at the fracture sites even when compacted at a pressure of 50 MPa

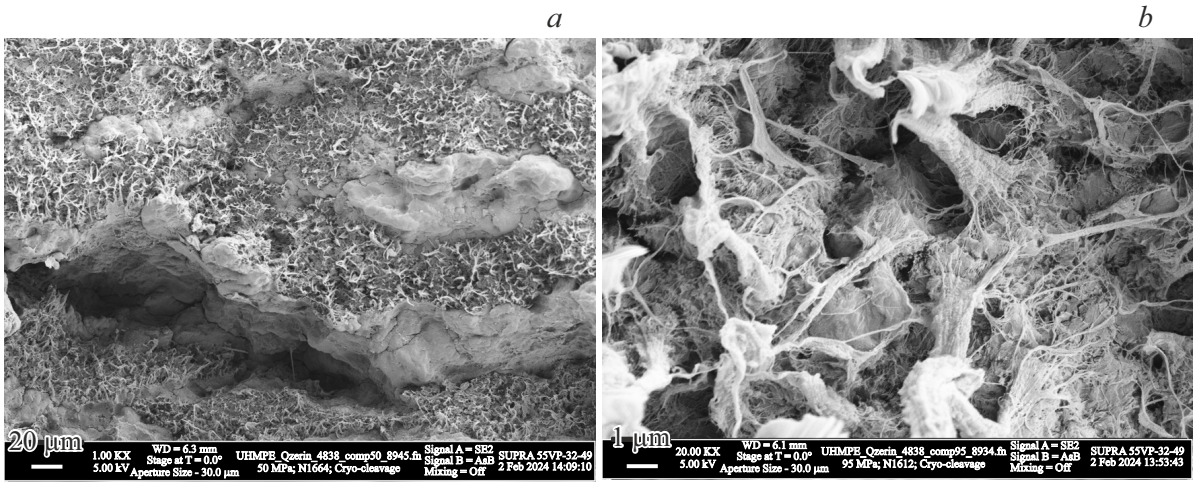

Figure 5. Cryo-cleavages of the compacts of the O4838 reactor powder, which are produced at the pressure of *a*) 50 MPa and *b*) 95 MPa.

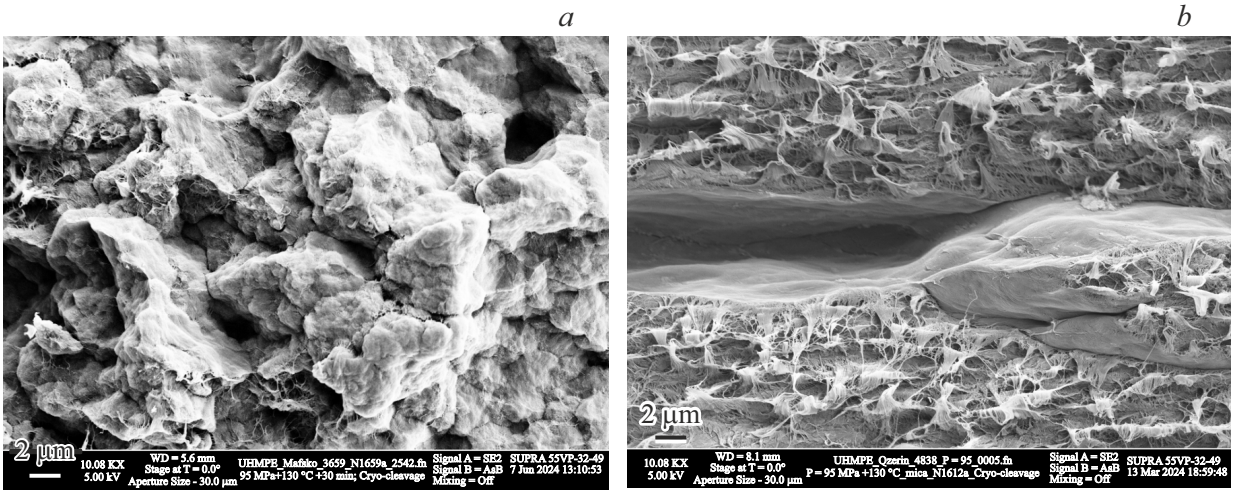

Figure 6. Cryo-cleavages of the samples sintered at 130 °C, *a*) M3659 and *b*) O4838.

(Figure 5, *a*). However, with higher magnifications, the cryo-cleavages of the samples compacted at the pressure of 95 MPa exhibit locations, in which a structure of the initial particles is observed. Apparently, these are the locations, in which white inclusions are visible on the transparent film and they indicate inhomogeneous compaction.

When examining the micrographs of the cryo-cleavages of the reactor powders sintered at the identical conditions ($T = 130\,^{\circ}\mathrm{C}$, $\mathrm{P} = 95$ MPa, the sintering time is 30 min), then an evident difference in the fracture structure is also observed (Figure 6).

After sintering of the O4838 compacts, a layered structure was formed and preserved a morphology of the compact, whereas spherical particles of the sintered M3659 compact became less smooth and were compacted without formation of layered cavities, in contrast to the sintered O4838 reactor powder.

It is important to note that the given micrographs are not a direct representation of the internal structure of the reactor powder. They are a result of interaction of a growing crack with the internal structure of the sample during breaking. Due to dulling and deceleration of the crack as a result of local plastic deformation of a material, a mechanism of cleavage surface relief formation can be different. With accumulation of energy, the crack can propagate for a certain distance and then can stop again. As a result of this, a collapsing surface can form „beads“, i. e. crack vertices. In some cases, a crack propagation speed can be up to the speed of sound, at which sufficient energy is released to remelt the sample fracture surface [18]. Therefore, interpretation of the micrographs of the cryo-cleavages should be approached with caution. Now, it is safe to say only one thing, i. e. a main crack propagates differently, which is apparently due to a significant difference of the structure in a volume of the

monolithized reactor powders synthesized on the various catalyst systems.

3.3. Plasma-induced thermoluminescence

As mentioned above, the thermoluminescence method allows obtaining unique information about molecular mobility (relaxation transitions) in the nearsurface nanolayers of the polymers. It is clear that the possibility of creating a high-quality mechanically coherent film from UHMWPE depends on molecular mobility.

Figure 7 shows glowing curves of the UHMWPE reactor powders O4838 and M3659 compacted at the various pressures.

It is clear that an increase of the compaction pressure in 2 times slightly changes total sum of luminescence of the compact (an area under the glowing curve) of the M3659 reactor powder with the dense globular structure (the curves *3* and *4*), whereas molecular mobility in the nearsurface nanolayers of the compact O4838 reactor powder with the flaky loose heterogeneous morphology noticeably decreases with an increase of the compaction pressure. Besides, all the glowing curves have a complicate profile, which makes to assume that several relaxation processes are overlapped, wherein a ratio of intensities of the low- and high-temperature peaks depends on the reactor powder type and the compaction pressure. Changes of the profiles of the glowing curves are also observed when investigating the sintered compacts in a dependence on the reactor powder type and the compact preparation conditions (Figure 8).

We note that sum of luminescence of the sintered samples is less as compared to that of the compacted samples. It indicates that sintering results in reduction of the number of defects on the surface of the precursors.

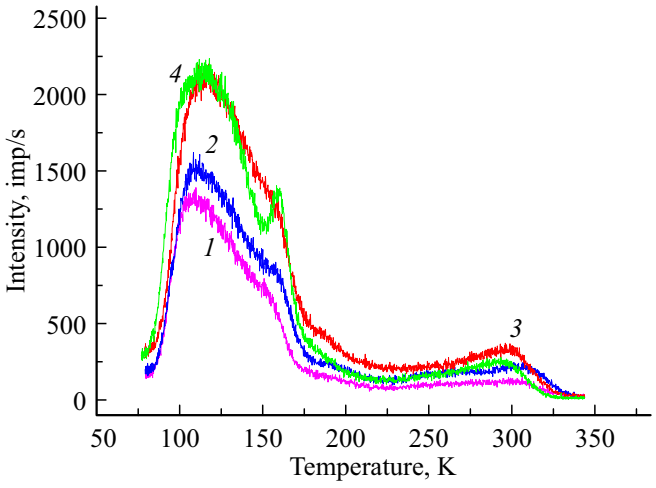

Figure 7. Glowing curves of the compacts produced at the pressure of 50 MPa (the O4838 reactor powder, the curve *1*, and the M3659 reactor powder, *3*) and at the pressure of 95 MPa (the O4838 reactor powder, *2*, and the M3659 reactor powder, *4*).

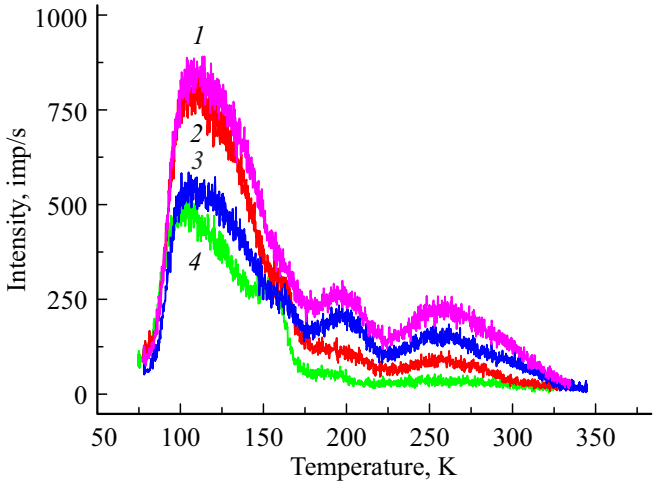

Figure 8. Glowing curves of the precursors sintered at the pressure of 95 MPa for 30 min at 130 °C from the compacts prepared at the various pressures: O4838 (the curve *1* — 50 MPa; *3* — 95 MPa) and M3659 (*2* — 50 MPa; *4* — 95 MPa).

It is known that the low-temperature peaks in the polyethylene within the range 90–130 K correspond to unfreezing of torsion oscillations of portions of chains in a scale of two or three monomer units that are localized near defects in the crystallites or in the disordered areas. The relaxation transitions within the temperature range 140–220 K are assigned to quasi-independent motion of segments of molecules (about ten monomer units) comparable with a Kuhn segment in the polyethylene (β-relaxation), while the transitions within the range 240–310 K already correspond to cooperative motion of these segments (α-relaxation) [19].

As said above, the complicate nature of the glowing curves of the studied samples makes it possible to assume that the experimental curves are a superposition of several relaxation processes that include erosion of electron traps. Decomposition of the experimental curves into elementary peaks would allow obtaining information about energy characteristics of these „elementary" processes and additional information concerning molecular dynamics of the surface layers of the nascent particles of the studied reactor powders. An issue of decomposition of the glowing curve into the elementary peaks is quite complicated. To a certain extent, decomposition is a quite voluntaristic procedure, since it is eventually unknown how many elementary relaxation processes occur within the studied temperature range.

All the glowing curves obtained from the compacted and sintered samples of the studied UHMWPE reactor powders could be decomposed into five or six maximums using the Fityk 1.0 software with a correlation factor of at least 0.99.

Figure 9 exemplifies one of the decompositions.

It has been previously shown that enhancement of luminescence at linear heating of the samples, which is observed in some temperature ranges, coincides with the

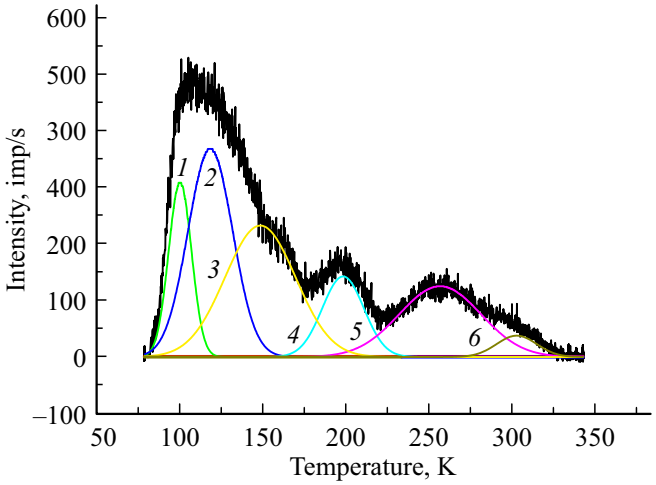

Figure 9. Decomposition of the glowing curve of the precursor sintered at the pressure of 95 MPa at 130 °C for 30 min from the O4838 compact that was produced by cold pressing at the pressure of 95 MPa, into the relaxation transitions: γ_1 (the curve *1*), γ_2 (*2*), β_1 (*3*), β_2 (*4*), α_1 (*5*), α_2 (*6*).

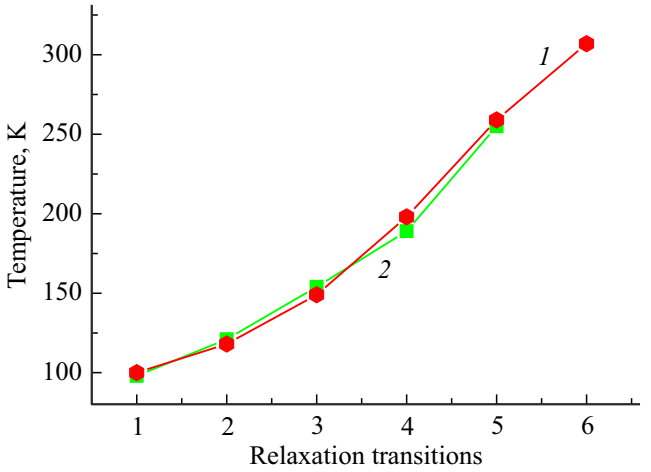

Figure 10. Comparison of the temperatures of the relaxation transitions in the precursors sintered at the pressure of 95 MPa at 130 °C for 30 min: the reactor powder O4838 (the curve *1*, the red one) and M3659 (*2*, the green one). The relaxation transitions are designated by digits on the Xaxis: 1 (γ_1), 2 (γ_2), 3 (β_1), 4 (β_2), 5 (α_1), 6 (α_2).

relaxation transitions in the material, which are recorded by other methods [18].

The process of the relaxation transitions includes destruction of the electron traps by thermal motion and release of „captured“ electrons from them. The released electrons migrate along the chain until they recombine with a parent or other counter ion, thereby resulting in excitation of a molecule and emission of a light quantum when it is returned to a ground energy level.

It follows from analysis of the decompositions of the glowing curves that the temperatures of all the α-, β-, γ-relaxation transitions in these sintered samples are almost the same (Figure 10).

The only exception is the O4838 sintered sample that demonstrates an additional high-temperature α_2-transition. It can be related to presence of long molecular segments involved in cooperative motion during unfreezing. It seems that the O4838 powders have a quite large number of longer molecular segments, for example, in a central part of the shish-kebabs, whose mobility is unfrozen when T exceeds 300 K. There are not shish-kebab formations in the M3659 reactor powder. In principle, knowing a temperature of destruction of the electron trap, it is possible to calculate a length of its constituent segments, which will be done further on.

However, despite identity of the temperatures of the relaxation transitions, the contribution by mobility of separate elements of the structure to total sum of luminescence of the sample can be different. A ratio of the area of each elementary peak to the total area of the glowing curve allows one to estimate the contribution by the respective relaxation transition to total sum of luminescence of the sample. We have evaluated it for the samples compacted at the various pressures (Figure 11) and for the sintered samples (Figure 12).

The results are analyzed to show that the contribution to total sum of luminescence by the M3659 powders compacted at 95 MPa is smaller than that by the O4838 compacts around the γ-transition, and is greater than that by the O4838 compacts around the α- and β-transitions.

After sintering, the ratios between these peaks change (Figure 12). The M3659 sintered samples have the contribution by γ relaxation β increased.

At first sight, this observation seems surprising. A question arises — why sintering results in increase of the smallest defects on the surface (ends of the molecules and separate atomic groups), although it would seem that

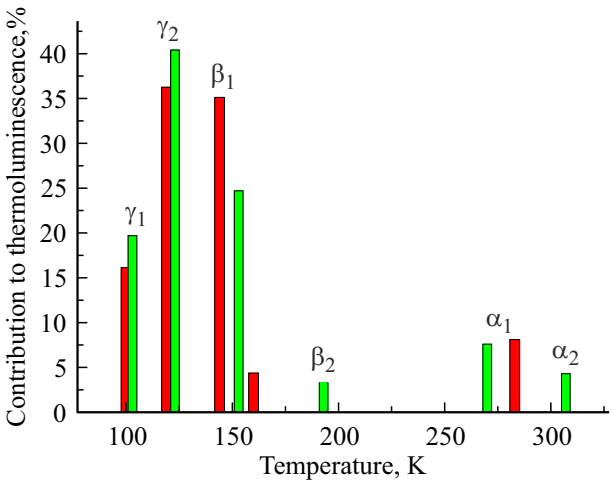

Figure 11. Contribution by the relaxation processes to molecular mobility in the nearsurface nanolayers of the reactor powders O4838 (the green columns) and M3659 (the red columns), which are compacted at 95 MPa.

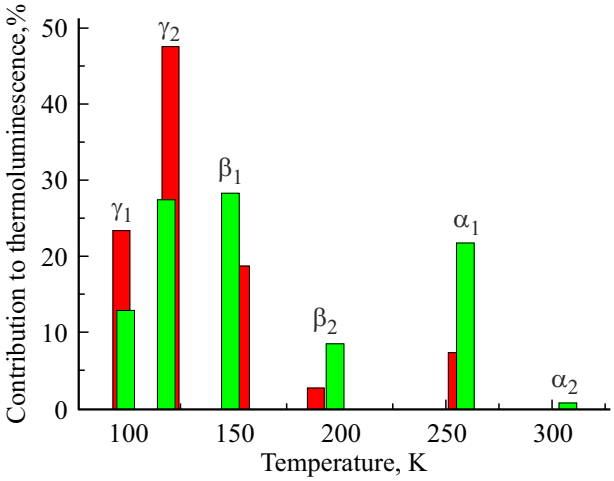

Figure 12. Contribution by the relaxation processes to molecular mobility in the nearsurface layers of the samples of the reactor powders M3659 (the red columns) and O4838 (the green columns), which are compacted at the pressure of 95 MPa and sintered at the same pressure at 130 °C.

sintering shall result in a more perfect state of the polymer surface. At the same time, the similar observations were obtained by us when comparative studying the surface of the polyethylene crystallized for a long time at the temperature close to the polyethylene melting temperature and the surface of the polyethylene quenched from a melt. It was found that the surface of the long-crystallized polyethylene has more defects than the surface of the quenched sample. It was assumed that during long crystallization defects were pushed out to the surface (the surface was devitrified). It seems that the similar effect takes place in this case, too. At the same time, on the contrary, in the O4838 sample the contribution by γ-relaxation to total sum of luminescence decreases, so does the contribution by α-relaxation, while the contribution by the β-relaxation increases. But now it is difficult to say which characteristics of the relaxation transitions and which ratio of their contributions to total mobility of the sample surface will provide high orientational elongations and, respectively, record mechanical characteristics of a finished product. This question will be answered only after strain hardening of the precursors, which is planned to be performed when using the multistage orientation zone drawing method. As of now, only comparative measurements of the strength of the precursors that are sintered for 30 min at the pressure of 95 MPa at 127 and 130 °C have been performed.

3.4. Mechanical tests

We did not manage to measure the strength of the precursors sintered at 127 °C, since they were broken in clamps. Only the strengths of the precursors sintered at 130 °C at the pressure of 95 MPa for 30 min were measured. Averaging was performed over 5–8 samples. The strength of the O4838 precursors of the reactor powder synthesized on the metallocene catalyst turned out to be somewhat higher (23.9 ± 0.9 MPa) the strength of M3659 of the reactor powder synthesized on the modified Ziegler TMC (21.5 ± 2.0 MPa), which can be explained by the large number of chain ends and short molecular segments in the subsurface nanolayers of the M3659 precursor. The observed difference in the strength is slight and requires more reliable statistical confirmation. The structural and mechanical characteristics of the precursors, which affect the properties of the finished product, can be evaluated in the future after orientational hardening.

4. Conclusion

The processes of monolithization of the reactor powders (RP) of ultra-high molecular weight polyethylene (UHMWPE), which are synthesized on the Ziegler-Natta and metallocene catalysts, have been comprehensively studied. The main focus was on investigating the influence of compaction and sintering conditions on the structural, thermal and mechanical properties of the produced precursors for subsequent strain hardening.

The study results have shown that the UHMWPE reactor powders synthesized on the metallocene catalyst demonstrate better ability to compaction and sintering as compared to the powders produced on the modified titanium-magnesium catalyst (TMC). It is confirmed by the higher strength of the precursors (23.9 MPa vs. 21.5 MPa) after sintering at the optimal conditions (130 °C, 95 MPa, 30 min). The analysis by differential scanning calorimetry has shown that the selected temperature sintering modes do not result in undesirable rearrangement of the initial structure of the polymer.

The studies by scanning electron microscopy revealed differences in the morphology of the powder particles: the powders synthesized on the metallocene catalyst are flake-shaped and consist of various morphoses. As we believe, it contributes to more intense shear strain during powder monolithization accompanied by formation of the cohesive bonds as compared to the TMC-based M3659 reactor powder, whose particles consist of the densely tightly globules.

Of particular interest are the data obtained by the plasma-induced thermoluminescence method, which allowed a detailed study of molecular mobility in the nearsurface nanolayers of the polymer.

The decomposition of glowing curves ($R^2 \geq 0.99$) by means of the Fityk software has shown that in the RP based on TMC (M3659) the contribution of β-relaxation predominates, whereas the metallocene powders (O4838) exhibited the additional α_2-transition (~ 307 K), which can be related to large variety of the morphological structures. After sintering, the glowing intensity decreases, thereby indicating reduction of the number of defects in the material. At the same time, the ratio of the contributions by theγ-, β-

and α-transitions changes, thereby indicating redistribution of molecular mobility in the nearsurface nanolayers.

A final conclusion concerning suitability of the reactor powder for solid-phase processing will be made only after results of orientational hardening. Based on analysis of the obtained data, one will be able to formulate a scientifically based mode of precursor production for orientational hardening.

Funding

Government budget. 29.19.04: Solid-state structure, 29.19.13: Mechanical properties of solid bodies.

Conflict of interest

The authors declare that they have no conflict of interest.

References

[1] Yu.I. Matveev, A.A. Askadskii. VMS B **36**, *10*, 1750 (1994). (in Russian).
[2] P.J. Lemstra, P. Smith. Brit. Poly. J. **12**, *4*, 212 (1980). https://doi.org/10.1002/pi.4980120415
[3] B.P. Rotzinger, H.D. Chanzy, P. Smith. Polymer **30**, *10*, 1814 (1989). https://doi.org/10.1016/0032-3861(89)90350-9
[4] H.D. Chanzy, B.P. Rotzinger, P. Smith. US Patent 4769433 (1988).
[5] S. Rastogi, K. Sharma, R. Duchateau, G.J.M. Gruter, D.R. Lippits. US Patent 0142521 (2006).
[6] S. Rastogi, Y. Yao, S. Ronca, J. Bos, J. van der Eem. Macromolecules **44**, *14*, 5558 (2011). https://pubs.acs.org/doi/10.1021/ma200667m
[7] A.N. Ozerin, S.S. Ivanchev, S.N. Chvalun, V.A. Aulov, N.S. Ivancheva, N.F. Bakeev. Polym. Sci. Ser. A **54**, *12*, 950 (2012).
[8] A.N. Ozerin, E.K. Golubeva, S.S. Ivanchev, V.A. Aulov, A.S. Kechek'yan, T.S. Kurkin, E.M. Ivan'kova, N.Yu. Adonin. VMS A **64**, *2*, 83 (2022). (in Russian).
[9] L.P. Myasnikova, V.A. Marikhin, A.K. Gladkov, O.Yu. Solov'eva, E.I. Radovanova, Yu.M. Boiko, E.M. Egorov. J. Phys.: Conf. Ser. **1697**, *1*, 012251 (2020). https://doi.org/10.1088/1742-6596/1697/1/012251
[10] V.F. Drobot'ko, L.P. Myasnikova, A.P. Borzenko, V.A. Marikhin, Yu.M. Boiko, V.M. Tkachenko, I.M. Makmak, N.E. Pis'menova, E.I. Radovanova, S.A. Terekhov. FTVD **33**, *2*, 86 (2023). (in Russian).
[11] M. Dermeneva, E. Ivan'kova, V. Marikhin, L. Myasnikova, M. Yagovkina, E. Radovanova. J. Phys.: Conf. Ser. **1038**, *1*, 012058 (2018). https://doi.org/10.1088/1742-6596/1038/1/012058
[12] T. Kanamoto, A. Tsuruta, K. Kanaka, M. Takeda, R.S. Porter. Polym. J. **15**, *4*, 327 (1983). https://doi.org/10.1295/polymj.15.327
[13] M.B. Konstantinopol'skaya, S.N. Chvalun, V.I. Selikhova, A.N. Ozerin, Yu.A. Zubov, N.F. Bakeev. VMS B **27**, *7*, 538 (1985). (in Russian).
[14] A.S. Maxwell, A.P. Unwin, I.M. Ward. Polymer **37**, *15*, 3293 (1996). https://doi.org/10.1016/0032-3861(96)88475-8
[15] A.A. Kalachev, N.M. Blashenkov, Yu.P. Ivanov, A.L. Myasnikov, L.P. Myasnikova, V.L. Koval'skii. Patent RF № 2112650 (2003). (in Russian).
[16] L.P. Myasnikova, N.M. Blashenkov, Yu.M. Boiko, E.M. Ivan'kova, A.A. Kalachev, D.V. Lebedev, V.A. Marikhin, E.I. Radovanova. Macromol. Symp. **242**, 182 (2006). https://doi.org/10.1002/masy.200651026
[17] P. Smith, H.D. Chanzy, B.P. Rotzinger. Polymer Commun. **26**, *9*, 258 (1985).
[18] O.F. Kireenko, V.A. Marikhin, L.P. Myasnikova. VMS A **1**, *1*, 30 (1981). (in Russian).
[19] I.V. Kuleshov, V.G. Nikol'skii. Radiotermolyuminestsentsiya polimerov. Khimiya, M. (1991). 123 s. (in Russian).

Translated by M.Shevelev